Purely irrotational theories of the effect of the viscosity on the decay of free gravity waves

J. Wang and D. D. Joseph

January, 2005

Abstract

A purely irrotational theory of the effect of viscosity on the decay of free gravity waves is derived and shown to be in excellent agreement with Lamb's (1932) exact solution. The agreement is achieved for all waves numbers k excluding a small interval around a critical $k=k_c$ where progressive waves change to monotonic decay. Very detailed comparisons are made between the purely irrotational and exact theory.

1. Introduction

Lamb (1932, §348, §349) performed an analysis of the effect of viscosity on free gravity waves. He computed the decay rate by a dissipation method using the irrotational flow only. He also constructed an exact solution for this problem, which satisfies both the normal and shear stress conditions at the interface.

Joseph and Wang (2004) studied Lamb's problem using the theory of viscous potential flow (VPF) and obtained a dispersion relation which gives rise to both the decay rate and wave-velocity. They also computed a viscous correction for the irrotational pressure and used this pressure correction in the normal stress balance to obtain another dispersion relation. This method is called a viscous correction of the viscous potential flow (VCVPF). Since VCVPF is an irrotational theory the shear stress cannot be made to vanish. However, the corrected pressure eliminates this uncompensated shear stress from the power of traction integral arising in an energy analysis of the irrotational flow.

Here we find that the viscous pressure correction of the irrotational motion gives rise to a higher order irrotational correction to the irrotational velocity which is proportional to the viscosity and does not have a boundary layer structure. The corrected velocity depends strongly on viscosity and is not related to vorticity; the whole package is purely irrotational. The corrected irrotational flow gives rise to a dispersion relation which is in splendid agreement with Lamb's exact solution, which has no explicit viscous pressure. The agreement with the exact solution holds for fluids even 10^4 times more viscous than water and for small and large wave numbers where the cutoff wave number k_c marks the place where progressive waves give rise to monotonic decay. We find that VCVPF gives rise to the same decay rate as in Lamb's exact solution and in his dissipation calculation when $k < k_c$. The exact solution agrees with VPF when $k > k_c$. The effects of vorticity are sensible only in a small interval centered on the cutoff wave number. We will do a comprehensive comparison for the decay rate and wave-velocity given by Lamb's exact solution and Joseph and Wang's VPF and VCVPF theories.

2. Irrotational viscous corrections for the potential flow solution

The gravity wave problem is governed by the continuity equation

$$\nabla \cdot \mathbf{u} = 0, \tag{1}$$

and the linearized Navier-Stokes equation

$$\frac{\partial \mathbf{u}}{\partial t} = -\frac{1}{\rho}\nabla p - g\mathbf{e}_y + \nu\nabla^2\mathbf{u}\,, \tag{2}$$

with the boundary conditions at the free surface ($y \approx 0$)

$$T_{xy} = 0\,, \qquad T_{yy} = 0\,, \tag{3}$$

where T_{xy} and T_{yy} are componets of the stress tensor and the surface tension is neglected. We divide the velocity and pressure field into two parts

$$\mathbf{u}=\mathbf{u}_\mathrm{p}+\mathbf{u}_\mathrm{v}, \qquad p=p_\mathrm{p}+p_\mathrm{v}, \tag{4}$$

where the subscript p denotes potential solutions and v denotes viscous corrections. The potential solutions satisfy

$$\mathbf{u}_\mathrm{p}= \nabla\phi\,, \qquad \nabla^2\phi = 0\,, \tag{5}$$

and

$$\frac{\partial \mathbf{u}_\mathrm{p}}{\partial t} = -\frac{1}{\rho}\nabla p_\mathrm{p} - g\mathbf{e}_y\,. \tag{6}$$

The viscous corrections are governed by

$$\nabla\cdot\mathbf{u}_\mathrm{v} = 0\,, \tag{7}$$

$$\frac{\partial \mathbf{u}_\mathrm{v}}{\partial t} = -\frac{1}{\rho}\nabla p_\mathrm{v} + \nu\nabla^2\mathbf{u}_\mathrm{v}\,. \tag{8}$$

We take the divergence of (8) and obtain

$$\nabla^2 p_\mathrm{v} = 0\,, \tag{9}$$

which shows that the pressure correction must be harmonic. Next we introduce a stream function ψ so that (7) is satisfied identically:

$$u_\mathrm{v} = -\frac{\partial\psi}{\partial y}\,, \qquad \mathrm{v}_\mathrm{v} = \frac{\partial\psi}{\partial x}\,. \tag{10}$$

We eliminate p_v from (8) by cross differentiation and obtain following equation for the stream function

$$\frac{\partial}{\partial t}\nabla^2\psi = \nu\nabla^4\psi\,. \tag{11}$$

To determine the normal modes which are periodic in respect of x with a prescribed wave-length $\lambda=2\pi/k$, we assume a time-factor e^{nt}, and a space-fact $\mathrm{e}^{\mathrm{i}kx}$

$$\psi = B\mathrm{e}^{nt+\mathrm{i}kx}\mathrm{e}^{my}\,, \tag{12}$$

where m is to be determined from (11). Inserting (12) into (11), we obtain

$$(m^2-k^2)\left[n-\nu(m^2-k^2)\right] = 0\,. \tag{13}$$

The root $m^2=k^2$ gives rise to irrotational flow; the root $m^2 = k^2 + n/\nu$ leads to the rotational component of the flow. The rotational component cannot give rise to a non-zero harmonic pressure because

$$\nabla^2\mathrm{e}^{nt+\mathrm{i}kx}\mathrm{e}^{my} = (m^2-k^2)\mathrm{e}^{nt+\mathrm{i}kx}\mathrm{e}^{my} \tag{14}$$

cannot vanish if $m^2 \neq k^2$. The only harmonic pressure for the rotational component is zero. Thus the governing equation for the rotational part of the flow can be written as

$$\frac{\partial\psi}{\partial t} = \nu\nabla^2\psi\,, \tag{15}$$

which is the equation used by Lamb (1932) in his exact solution.

The effect of viscosity on the decay of a free gravity wave can be approximated by a purely irrotational theory in which the explicit dependence of the power of traction of the irrotational shear stress is eliminated by a viscous contribution p_v to irrotational pressure. In this theory $\mathbf{u}=\nabla\phi$ and a stream function, which is associated with vorticity, is not introduced. The kinetic energy, potential energy and dissipation of the flow can be computed using the potential flow solution

$$\phi = A\mathrm{e}^{nt+ky+\mathrm{i}kx}. \tag{16}$$

We insert the potential flow solution into the mechanical energy equation

$$\frac{\mathrm{d}}{\mathrm{d}t}\left(\int_V \rho|\mathbf{u}|^2/2\,\mathrm{d}V + \int_0^\lambda \rho g\eta^2/2\,\mathrm{d}x\right) = \int_0^\lambda \left[\mathrm{v}(-p+\tau_{yy}) + u\tau_{xy}\right]\mathrm{d}x + \int_V 2\mu\mathbf{D}:\mathbf{D}\,\mathrm{d}V\,, \tag{17}$$

where η is the elevation of the surface and $\mathbf{D}$ is the rate of strain tensor. Motivated by previous authors (Moore 1963, Kang and Leal 1988), we add a pressure correction to the normal stress which satisfies

$$\int_0^\lambda \mathrm{v}(-p_\mathrm{v})\,\mathrm{d}x = \int_0^\lambda u\tau_{xy}\,\mathrm{d}x\,, \tag{18}$$

But in our problem here, there is no explicit viscous pressure function in the exact solution [see (24) and (25)]. It turns out that the pressure correction defined here in the purely irrotational flow is related to quantities in the exact solution in a complicated way which requires further analysis [see (31)].

Joseph and Wang (2004) solved for the harmonic pressure correction from (9), then determined the constant in the expression of p_v using (18), and obtained

$$p_\mathrm{v} = -2\mu k^2 A\mathrm{e}^{nt+ky+\mathrm{i}kx}. \tag{19}$$

The velocity correction associated with this pressure correction can be solved from (8). We seek normal modes solution $\mathbf{u}_\mathrm{v} \sim \mathrm{e}^{nt+ky+\mathrm{i}kx}$ and equation (8) becomes

$$\rho n\mathbf{u}_\mathrm{v} = -\nabla p_\mathrm{v}. \tag{20}$$

Hence, curl($\mathbf{u}_\mathrm{v}$) = 0 and $\mathbf{u}_\mathrm{v}$ is irrotational. After assuming $\mathbf{u}_\mathrm{v} = \nabla\phi_1$ and $\phi_1 = A_1\mathrm{e}^{nt+ky+\mathrm{i}kx}$, we obtain

$$\rho n\phi_1 = -p_\mathrm{v} \quad \Rightarrow \quad \phi_1 = \frac{2\mu k^2}{\rho n}A\mathrm{e}^{nt+ky+\mathrm{i}kx}. \tag{21}$$

We compute the viscous normal stress due to the velocity correction

$$2\mu\frac{\partial \mathrm{v}_\mathrm{v}}{\partial y} = 2\mu\frac{\partial^2\phi_1}{\partial y^2} = \frac{4\mu^2k^4}{\rho n}A\mathrm{e}^{nt+ky+\mathrm{i}kx}. \tag{22}$$

Since for mobile fluids such as water or even glycerin, $\nu=\mu/\rho$ is small, this viscous normal stress is negligible compared to p_v when k is small. Therefore, the viscous normal stress induced by the velocity correction can be neglected in the normal stress balance in the VPVPF theory. The viscous normal stress (22) could be large when k is large, however, we will show in the following sections that the flow is nearly irrotational at large values of k and no correction is needed.

The calculation shows that the velocity correction $\mathbf{u}_v$ associated with the pressure correction is irrotational. Our pressure correction (19) is proportional to μ and on the same order of the viscous stresses evaluated using ϕ (16). This pressure correction is associated with a correction for the velocity potential ϕ_1 (21), which is also proportional to μ. The shear stress evaluated using ϕ_1 is proportional to μ^2 and non-zero. To balance

the power of this non-physical shear stress, one can add a pressure correction proportional to μ^2, which will in turn induce a correction for the velocity potential proportional to μ^2. One can continue to build higher order corrections and they will all be irrotational. The final velocity potential has the following form

$$\phi = (A + A_1 + A_2 + \cdots)\mathrm{e}^{nt+ky+\mathrm{i}kx}, \tag{23}$$

where $A_1 \sim \mu$, $A_2 \sim \mu^2$... Thus the VCVPF theory is an approximation to the exact solution based on solely potential flow solutions. The higher order corrections are small for liquids with small viscosities; the most important correction is the first pressure correction proportional to μ. In our application of VCPVF to the gravity wave problem, only the first pressure correction (19) is added to the normal stress balance and higher order normal stress terms such as (22) are not added. We obtain a dispersion relation in excellent agreement with Lamb's exact solution (see the comparison in the next section); adding the higher order corrections to the normal stress balance does not improve the VCVPF approximation. It should be pointed out that no matter how many correction terms are added to the potential (23), the shear stress evaluated using (23) is still non-zero unless $(A + A_1 + A_2 + ...) = 0$. Therefore, VCVPF is only an approximation to the exact solution and cannot satisfy the shear stress condition at the free surface.

Prosperetti (1976) considered viscous effects on standing free gravity waves using the same governing equations (7) and (8) for the viscous correction terms. If we adapt our VCPVF method to treat standing waves represented by the potential $\phi = k^{-1}(\mathrm{da/dt})\mathrm{e}^{ky}\cos kx$, we can obtain $-p_{\mathrm{v}} = 2\mu k(\mathrm{da/dt})\mathrm{e}^{ky}\cos kx$, which is exactly the same pressure correction obtained by Prosperetti (1976) using a different method.

3. Relation between the pressure correction and Lamb's exact solution

In Lamb's exact solution, the solution is given by a potential ϕ and a stream function ψ:

$$u = \frac{\partial\phi}{\partial x} - \frac{\partial\psi}{\partial y}, \qquad \mathrm{v} = \frac{\partial\phi}{\partial y} + \frac{\partial\psi}{\partial x}, \qquad \frac{p}{\rho} = -\frac{\partial\phi}{\partial t} - gy, \tag{24}$$

provided

$$\nabla^2\phi = 0, \qquad \partial\psi/\partial t = \nu\nabla^2\psi. \tag{25}$$

The stream function gives rise to the rotational part of the flow. No pressure term enters into the stream function equation, as we have shown in the previous section that the only harmonic pressure for the rotational part is zero. The pressure p comes from Bernoulli's equation in (24) and no explicit viscous pressure exists, though p depends on the viscosity through the velocity potential. Lamb shows that (25) can be solved with normal modes

$$\phi = A\mathrm{e}^{ky}\mathrm{e}^{\mathrm{i}kx+nt}, \qquad \psi = C\mathrm{e}^{my}\mathrm{e}^{\mathrm{i}kx+nt}, \qquad m^2 = k^2 + n/\nu, \tag{26}$$

where A and C are constants.

We derive the connection between the viscous pressure correction p_{v} in our VCVPF theory and Lamb's exact solution in which no explicit viscous pressure exists. In the ensuring part of this section, superscript L represents Lamb's exact solution and J represent Joseph and Wang's VCVPF theory. The irrotational pressure in the two solutions are

$$p^E = -\rho\frac{\partial\phi^E}{\partial t} - \rho g\eta^E \ , \qquad p_{\rm i}^J = -\rho\frac{\partial\phi^J}{\partial t} - \rho g\eta^J \ . \tag{27}$$

The elevation η is obtained from the kinematic condition at $y \approx 0$

$$\frac{\partial\eta^E}{\partial t} = \frac{\partial\phi^E}{\partial y} + \frac{\partial\psi^E}{\partial x} \ , \ \frac{\partial\eta^J}{\partial t} = \frac{\partial\phi^J}{\partial y} \ . \tag{28}$$

The normal stress balance condition in the two solutions is respectively

$$T_{yy}^E = -p^E + 2\mu\frac{\partial^2\phi^E}{\partial^2 y} + 2\mu\frac{\partial^2\psi^E}{\partial x\partial y} = 0 \ , \tag{29}$$

$$T_{yy}^J = -p_{\rm i}^J - p_{\rm v} + 2\mu\frac{\partial^2\phi^J}{\partial^2 y} = 0 \ . \tag{30}$$

Therefore $T_{yy}^E - T_{yy}^J = 0$ and we can obtain

$$\frac{p_{\rm v}}{\rho} = \frac{\partial\left(\phi^J - \phi^E\right)}{\partial t} + g(\eta^J - \eta^E) + 2\nu\frac{\partial^2\left(\phi^J - \phi^E\right)}{\partial y^2} - 2\nu\frac{\partial^2\psi^E}{\partial x\partial y} \ . \tag{31}$$

This shows that the pressure correction in VCVPF is given by terms involving the potential part of Lamb's solution (different than VCVPF), the surface elevation in Lamb's solution (different than VCVPF) and the vortical part associated with the stream function in Lamb's solution.

To illustrate the contribution to $p_{\rm v}$ from each term in (31), we compute each term in (31) for SO10000 oil at different wave numbers. SO10000 oil has a kinematic viscosity 1.03×10^{-2} m^2/s, which is 10^4 times more viscous than water. Note that the amplitude A for the potential is different in Lamb's exact solution and in VCPVF:

$$\phi^E = A^E{\rm e}^{nt+ky+{\rm i}kx} \ , \qquad \phi^J = A^J{\rm e}^{nt+ky+{\rm i}kx}, \qquad A^E \neq A^J. \tag{32}$$

To make the two solutions comparable, we compute the relation between A^E and A^J by equating the dissipation evaluated using Lamb's exact solution and evaluated using VCVPF. In Table 1 we list the values of each term in (31) normalized by A^E. It seems that the term $g(\eta^J - \eta^E)$ gives the most important contribution to $p_{\rm v}$, but the other terms are not negligible.

k	$p_{\rm v}/\rho$	term1	term2	term3	term4
0.01	-2.063×10^{-6}	-1.325×10^{-9} + i0.000201	-2.063×10^{-6} – i0.000201	-1.325×10^{-9}	5.300×10^{-9} + i5.300×10^{-9}
0.1	-2.057×10^{-4}	-7.441×10^{-7} + i0.00358	-2.071×10^{-4} – i0.00358	-7.461×10^{-7}	2.980×10^{-6} + i2.980×10^{-6}
1	–0.02022	-4.207×10^{-4} + i0.06272	–0.02106 – i0.06440	-4.186×10^{-4}	0.001679 + i0.001679
10	–1.881	–0.3131 + i0.6303	–2.423 – i1.513	–0.1829	1.038 + i0.8830

Table 1. The value of each term in (31) normalized by A^E for SO10000 oil at different wave numbers; term1 = $\partial\left(\phi^J - \phi^E\right)/\partial t$, term2 = $g(\eta^J - \eta^E)$, term3 = $2\nu\partial^2\left(\phi^J - \phi^E\right)/\partial y^2$, and term4 = $2\nu\partial^2\psi^E/\partial x\partial y$.

4. Comparison of the decay rate and wave-velocity given by the exact solution, VPF and VCVPF

When the surface tension is ignored, Lamb's exact solution gives rise to the following dispersion relation:

$$n^2 + 4\nu k^2 n + 4\nu^2 k^4 + gk = 4\nu^2 k^3 \sqrt{k^2 + n/\nu} \ . \tag{33}$$

Lamb considered the solution of (33) at limits of small k and large k. When $k << k_c = (g/\nu^2)^{1/3}$, he obtained approximately

$$n = -2\nu k^2 \pm \mathrm{i} k\sqrt{g/k} \ , \tag{34}$$

which gives rise to the decay rate $-2\nu k^2$, in agreement with the dissipation result, and the wave-velocity $\sqrt{g/k}$, which is the same as the wave-velocity for inviscid potential flow. When $k >> k_c = (g/\nu^2)^{1/3}$, Lamb noted that the two roots are both real. One of them is

$$n_1 = -\frac{g}{2\nu k} \ , \tag{35}$$

and the other one is

$$n_2 = -0.91\nu k^2 \ . \tag{36}$$

Lamb pointed out n_1 is the more important root because the motion corresponding to n_2 dies out very rapidly.

Basset (1896) commented on the exact solution "These results are entirely in accordance with what is observed in the case of viscous liquids. If for examples a jet of air were directed for a short time to the surface of a slightly viscous liquid such as water, waves would be observed to diverge from the point of application of the jet, whose amplitudes gradually diminish as the time advances, until the motion ultimately dies away. But if the jet were applied to the surface of a highly viscous liquid such as treacle of glycerine, waves would not be excited. The immediate effect of the jet of air would be to produce a depression in the neighbourhood of its point of application, and as soon as it had ceased, the liquid would sluggishly move so as to fill up the depression, and would very soon come to rest."

Joseph and Wang (2004) treated this problem using viscous potential flow and obtained

$$n^2 + 2\nu k^2 n + gk = 0 \, , \tag{37}$$

which is the dispersion relation for VPF theory. When $k < k_c = (g/\nu^2)^{1/3}$, the solution of (37) is

$$n = -\nu k^2 \pm \mathrm{i} k\sqrt{g/k - \nu^2 k^2} \ . \tag{38}$$

We note that the decay rate $-\nu k^2$ is half of that in (34) and the wave-velocity $\sqrt{g/k - \nu^2 k^2}$ is slower than the inviscid wave-velocity. When $k > k_c = (g/\nu^2)^{1/3}$, the two roots of (37) are both real and they are

$$n = -\nu k^2 \pm \sqrt{\nu^2 k^4 - gk} \ . \tag{39}$$

If $k >> k_c = (g/\nu^2)^{1/3}$, the above two roots are approximately

$$n_1 = -\frac{g}{2\nu k} \ , \tag{40}$$

and

$$n_2 = -2\nu k^2 + \frac{g}{2\nu k} \ . \tag{41}$$

We note that (40) is the same as (35), and the magnitude of (41) is approximately twice of (36).

Joseph and Wang (2004) computed a pressure correction and added it to the normal stress balance to obtain

$$n^2 + 4\nu k^2 n + gk = 0\,, \tag{42}$$

which is the dispersion relation for VCVPF theory. When $k < k'_c = (g/4\nu^2)^{1/3}$, the solution of (42) is

$$n = -2\nu k^2 \pm \mathrm{i}k\sqrt{g/k - 4\nu^2 k^2}\ . \tag{43}$$

We note that the decay rate $-2\nu k^2$ is the same as in (34) and the wave-velocity $\sqrt{g/k - 4\nu^2 k^2}$ is slower than the inviscid wave-velocity. When $k > k'_c = (g/4\nu^2)^{1/3}$, the two roots of (42) are both real and they are

$$n = -2\nu k^2 \pm \sqrt{4\nu^2 k^4 - gk}\ . \tag{44}$$

If $k >> k'_c = (g/4\nu^2)^{1/3}$, the above two roots are approximately

$$n_1 = -\frac{g}{4\nu k}\ , \tag{45}$$

and

$$n_2 = -4\nu k^2 + \frac{g}{4\nu k}\ . \tag{46}$$

We note that (45) is half of (35), and the magnitude of (46) is approximately four times of (36).

We compute the solution of (33) and compare the real and imaginary part of n with those obtained by solving (37) and (42). In figures 1, 2 and 3, we compare n for water, glycerin and SO10000 oil, respectively. The kinematic viscosity for water, glycerin and SO10000 oil is 10^{-6}, 6.21×10^{-4}, and 1.03×10^{-2} m^2/s, respectively. We show the results for ν= 10 m^2/s in figure 4, which is 1000 times more viscous than SO10000 oil; the comparison between the exact solution and VPF, VCVPF is still excellent. The cutoff wave number $k_c = (g/\nu^2)^{1/3}$ decreases as the viscosity increases. In Table 2 we list the values of k_c for water, glycerin, SO10000 oil and the liquid with ν= 10 m^2/s. In practice waves associated with different wave numbers may exist simultaneously. For very viscous fluids, k_c is small and the majority of the wave numbers are above k_c, therefore the motion of monotonic decay dominates; for less viscous fluids, the motion of progressive waves may dominate.

Fluid	water	glycerin	SO10000	-
ν(m^2/s)	10^{-6}	6.21×10^{-4}	1.03×10^{-2}	10
k_c(1/m)	21399.7	294.1	45.2	0.461

Table 2. The values for the cutoff wave number k_c for water, glycerin, SO10000 oil and the liquid with ν= 10 m^2/s. k_c decreases as the viscosity increases.

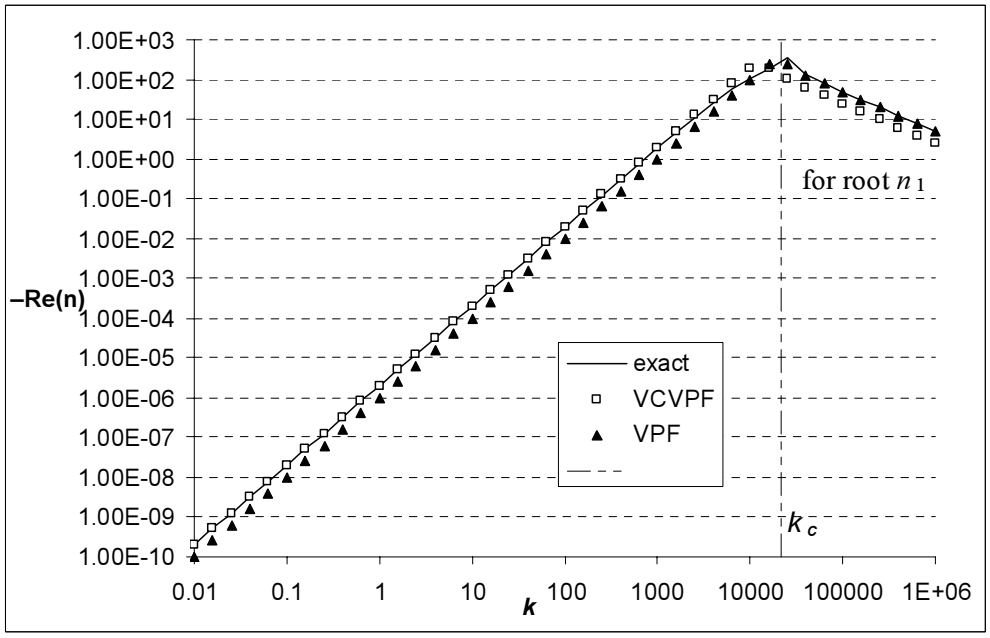

Figure 1. (a) Decay rate –Re(n) vs. wave number k for water, $\nu = 10^{-6}$ m^2/s. Re(n) is computed for the exact solution from (33), for VPF from (37) and for VCVPF from (42). When $k < k_c$, the decay rate $-2\nu k^2$ for VCVPF is in good agreement with the exact solution, whereas the decay rate $-\nu k^2$ for VPF is only half of the exact solution. When $k > k_c$, n has two real solutions in each theory. In this figure, we plot the decay rate n_1 corresponding to (35), (40) and (45). The exact solution can be approximated by $-g/(2\nu k)$; the decay rate $-g/(2\nu k)$ for VPF is in agreement with the exact solution, whereas the decay rate $-g/(4\nu k)$ for VCVPF is only half of the exact solution.

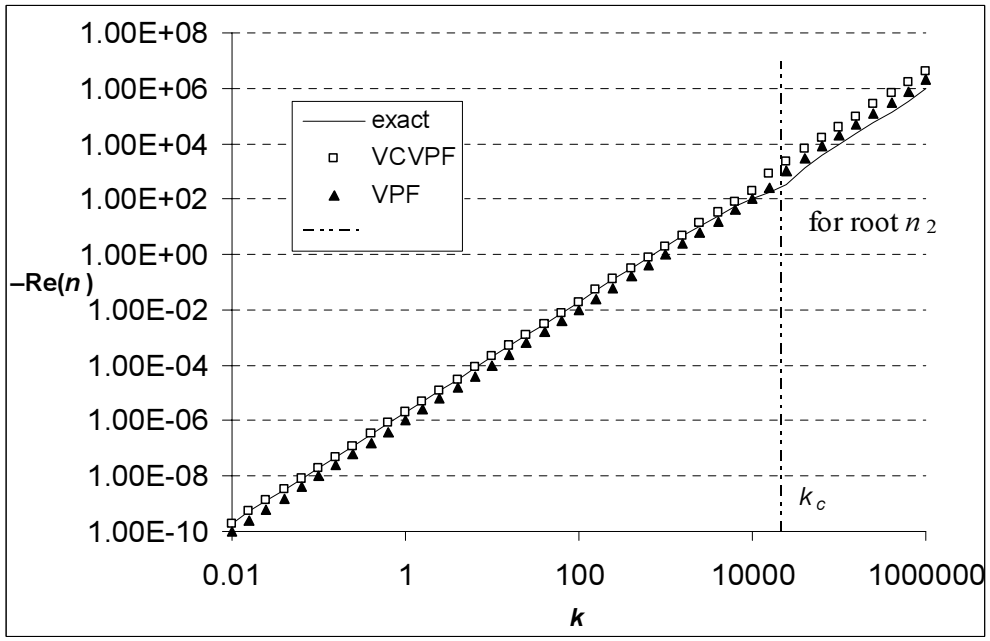

Figure 1. (b) Decay rate –Re(n) vs. wave number k for water, $\nu = 10^{-6}$ m^2/s. Re(n) is computed for the exact solution from (33), for VPF from (37) and for VCVPF from (42). When $k > k_c$, n has two real solutions in each theory. In this figure, we plot the decay rate n_2 corresponding to (36), (41) and (46). The decay rate for the exact solution can be approximated by $-0.91\nu k^2$; the decay rate $\approx -2\nu k^2$ for VPF is closer to the exact solution than the decay rate $\approx -4\nu k^2$ for VCVPF.

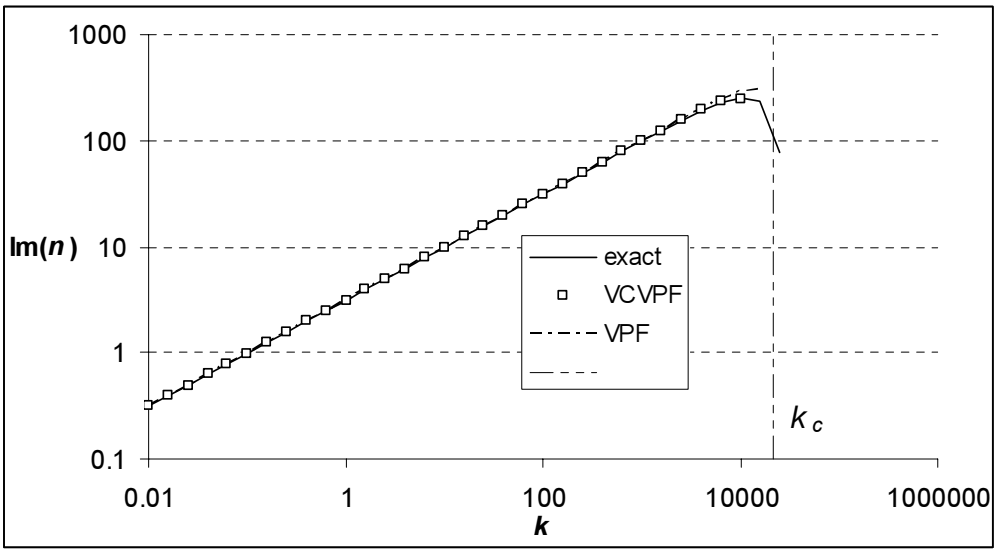

Figure 1. (c) Im(n), i.e. the wave-velocity multiplied by k, vs. wave number k for water, $\nu = 10^{-6}$ m^2/s. Im(n) is computed for the exact solution from (33), for VPF from (37) and for VCVPF from (42). When $k < k_c$, the three theories give almost the same wave-velocity. When $k > k_c$, all the three theories give zero imaginary part of n.

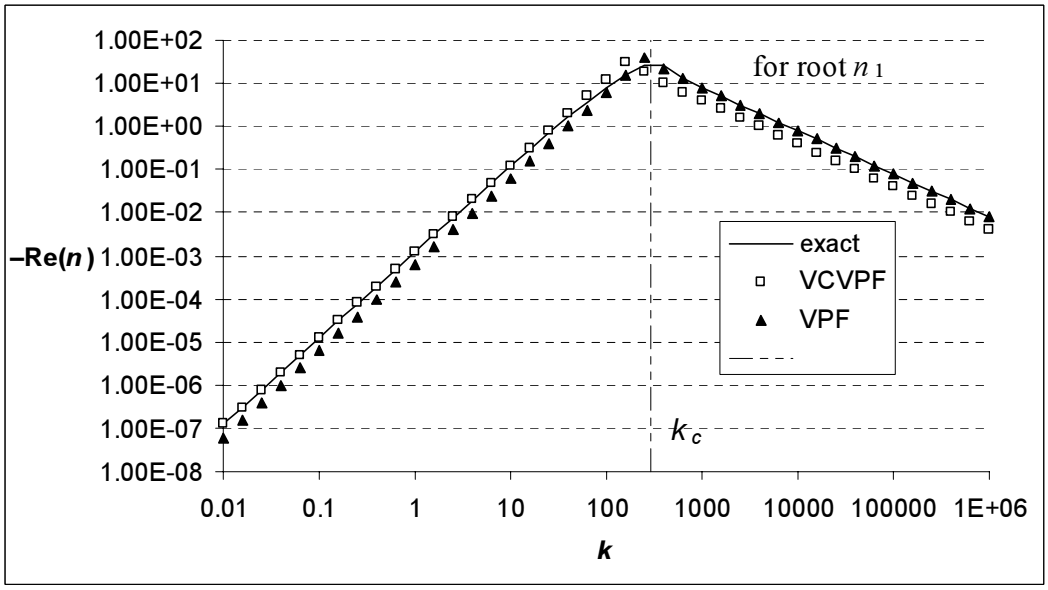

Figure 2. (a) Decay rate –Re(n) vs. wave number k for glycerin, $\nu = 6.21\times10^{-4}$ m^2/s. Re(n) is computed for the exact solution from (33), for VPF from (37) and for VCVPF from (42). When $k < k_c$, the decay rate $-2\nu k^2$ for VCVPF is in good agreement with the exact solution, whereas the decay rate $-\nu k^2$ for VPF is only half of the exact solution. When $k > k_c$, n has two real solutions in each theory. In this figure, we plot the decay rate n_1 corresponding to (35), (40) and (45). The decay rate for the exact solution can be approximated by $-g/(2\nu k)$; the decay rate $-g/(2\nu k)$ for VPF is in agreement with the exact solution, whereas the decay rate $-g/(4\nu k)$ for VCVPF is only half of the exact solution.

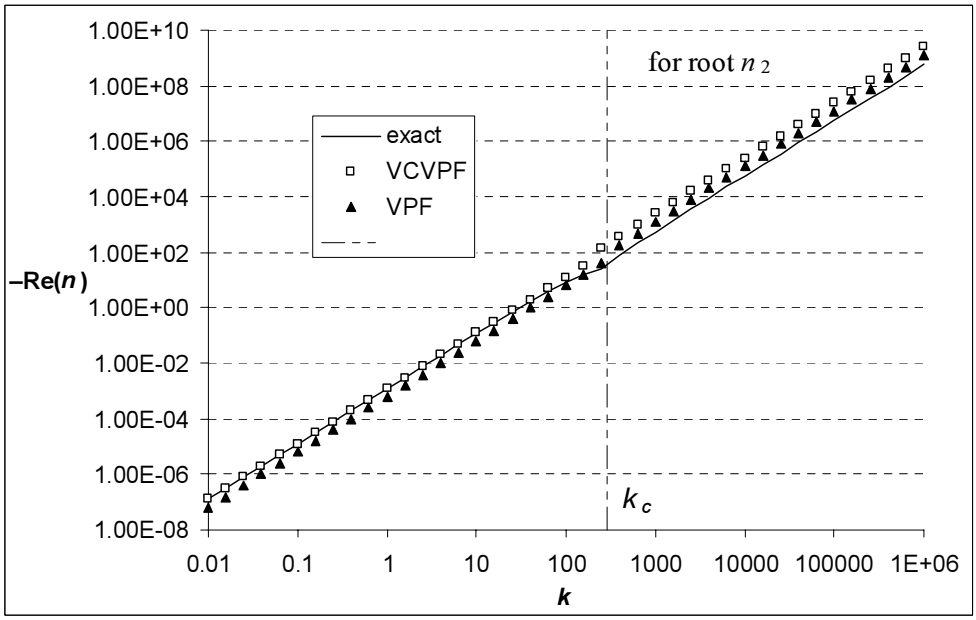

Figure 2. (b) Decay rate –Re(n) vs. wave number k for glycerin, $\nu = 6.21\times10^{-4}$ m^2/s. Re(n) is computed for the exact solution from (33), for VPF from (37) and for VCVPF from (42). When $k > k_c$, n has two real solutions in each theory. In this figure, we plot the decay rate n_2 corresponding to (36), (41) and (46). The decay rate for the exact solution can be approximated by $-0.91\nu k^2$; the decay rate $\approx -2\nu k^2$ for VPF is closer to the exact solution than the decay rate $\approx -4\nu k^2$ for VCVPF.

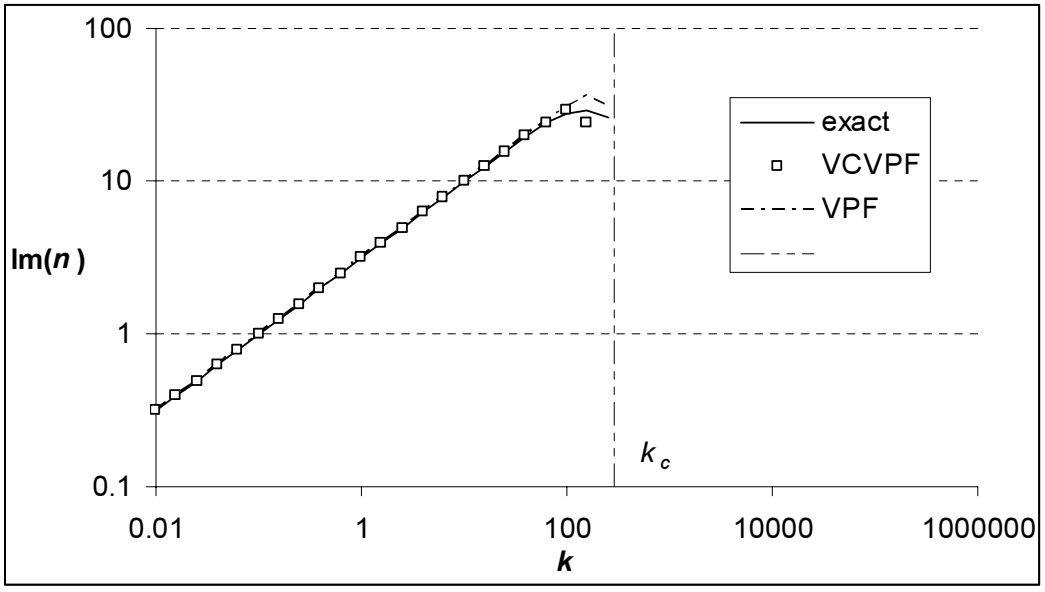

Figure 2. (c) Im(n), i.e. wave-velocity multiplied by k, vs. wave number k for glycerin, $\nu = 6.21\times10^{-4}$ m^2/s. Im(n) is computed for the exact solution from (33), for VPF from (37) and for VCVPF from (42). When $k < k_c$, the three theories give almost the same wave-velocity. When $k > k_c$, all the three theories give zero imaginary part of n.

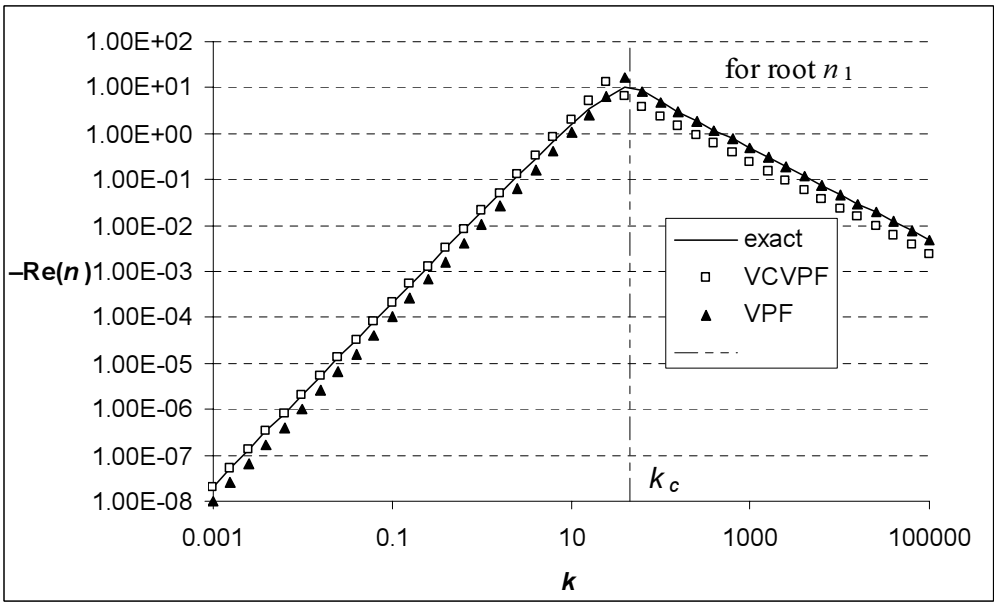

Figure 3. (a) Decay rate –Re(n) vs. wave number k for SO10000 oil, $\nu = 1.03\times10^{-2}$ m^2/s. Re(n) is computed for the exact solution from (33), for VPF from (37) and for VCVPF from (42). When $k < k_c$, the decay rate $-2\nu k^2$ for VCVPF is in good agreement with the exact solution, whereas the decay rate $-\nu k^2$ for VPF is only half of the exact solution. When $k > k_c$, n has two real solutions in each theory. In this figure, we plot the decay rate n_1 corresponding to (35), (40) and (45). The decay rate for the exact solution can be approximated by $-g/(2\nu k)$; the decay rate $-g/(2\nu k)$ for VPF is in agreement with the exact solution, whereas the decay rate $-g/(4\nu k)$ for VCVPF is only half of the exact solution.

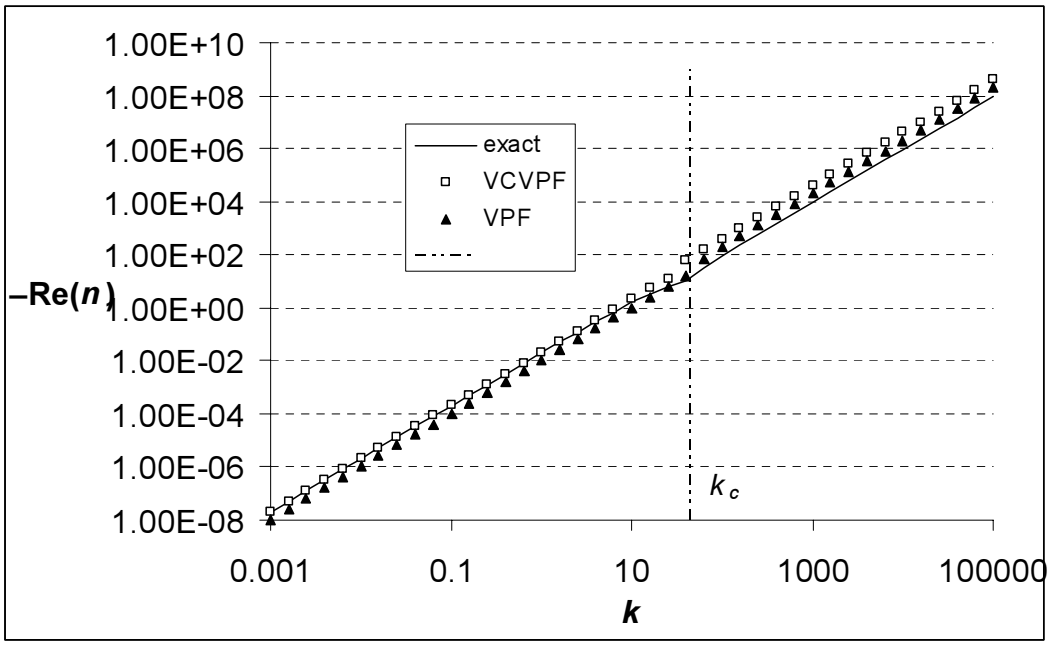

Figure 3. (b) Decay rate –Re(n) vs. wave number k for SO10000 oil, $\nu = 1.03\times10^{-2}$ m^2/s. Re(n) is computed for the exact solution from (33), for VPF from (37) and for VCVPF from (42). When $k > k_c$, n has two real solutions in each theory. In this figure, we plot the decay rate n_2 corresponding to (36), (41) and (46). The decay rate for the exact solution can be approximated by $-0.91\nu k^2$; the decay rate $\approx -2\nu k^2$ for VPF is closer to the exact solution than the decay rate $\approx -4\nu k^2$ for VCVPF.

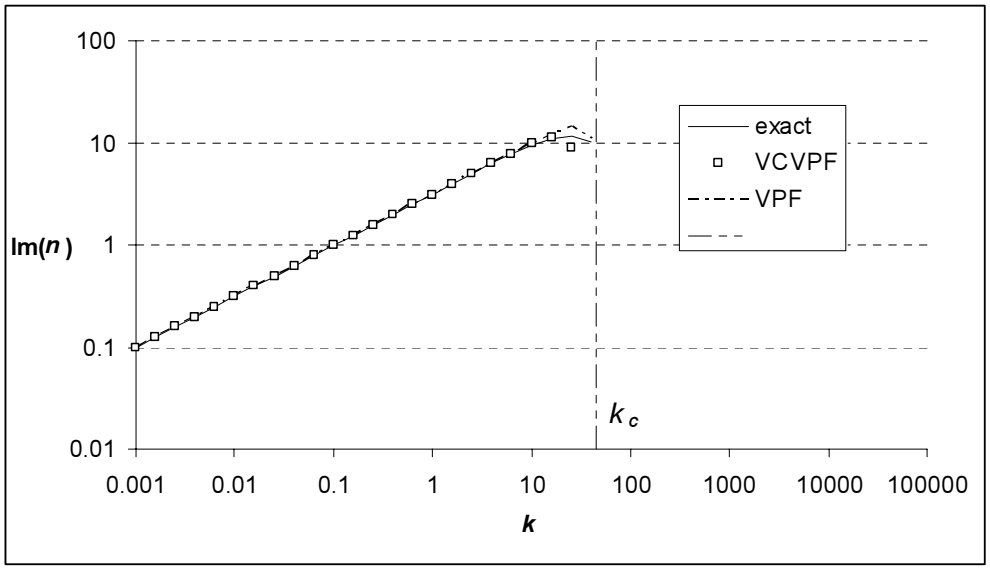

Figure 3. (c) Im(n), i.e. wave-velocity multiplied by k, vs. wave number k for SO10000 oil, $\nu = 1.03\times10^{-2}$ m^2/s. Im(n) is computed for the exact solution from (33), for VPF from (37) and for VCVPF from (42). When $k < k_c$, the three theories give almost the same wave-velocity. When $k > k_c$, all the three theories give zero imaginary part of n.

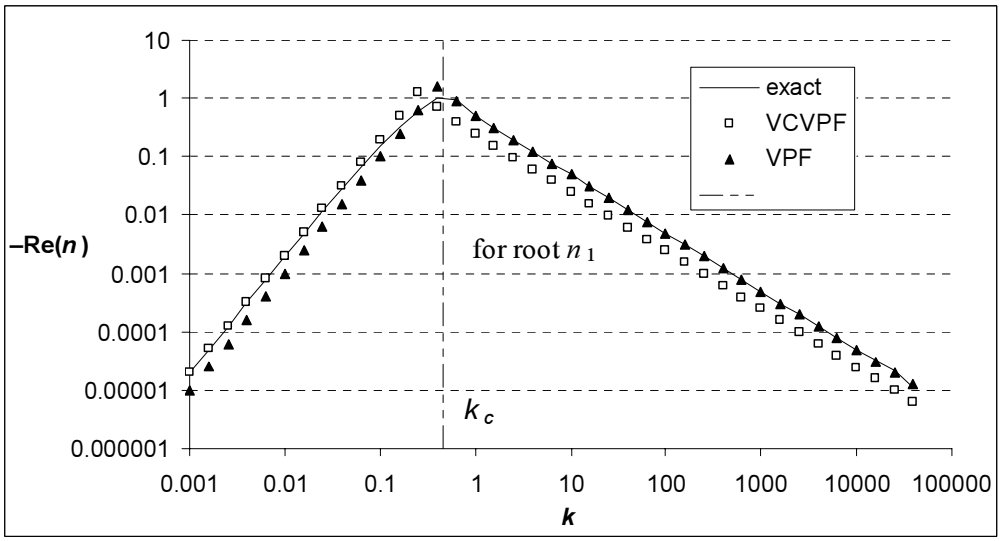

Figure 4. (a) Decay rate –Re(n) vs. wave number k for $\nu = 10$ m^2/s. Re(n) is computed for the exact solution from (33), for VPF from (37) and for VCVPF from (42). When $k < k_c$, the decay rate $-2\nu k^2$ for VCVPF is in good agreement with the exact solution, whereas the decay rate $-\nu k^2$ for VPF is only half of the exact solution. When $k > k_c$, n has two real solutions in each theory. In this figure, we plot the decay rate n_2 corresponding to (35), (40) and (45). The decay rate for the exact solution can be approximated by $-g/(2\nu k)$; the decay rate $-g/(2\nu k)$ for VPF is in agreement with the exact solution, whereas the decay rate $-g/(4\nu k)$ for VCVPF is only half of the exact solution.

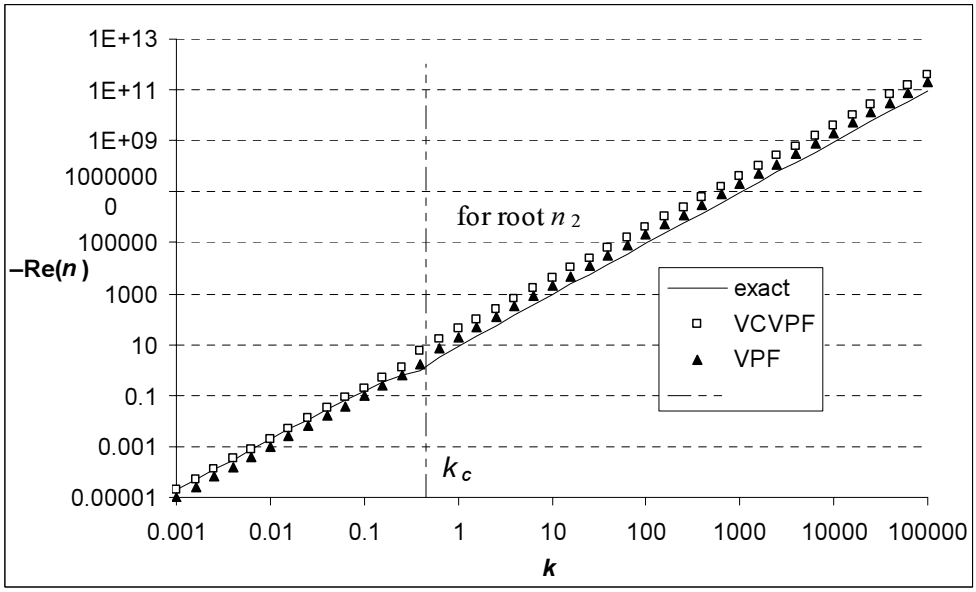

Figure 4. (b) Decay rate –Re(n) vs. wave number k for ν =10 m^2/s. Re(n) is computed for the exact solution from (33), for VPF from (37) and for VCVPF from (42). When $k > k_c$, n has two real solutions in each theory. In this figure, we plot the decay rate n_2 corresponding to (36), (41) and (46). The decay rate for the exact solution can be approximated by $-0.91\nu k^2$; the decay rate $\approx -2\nu k^2$ for VPF is closer to the exact solution than the decay rate $\approx -4\nu k^2$ for VCVPF.

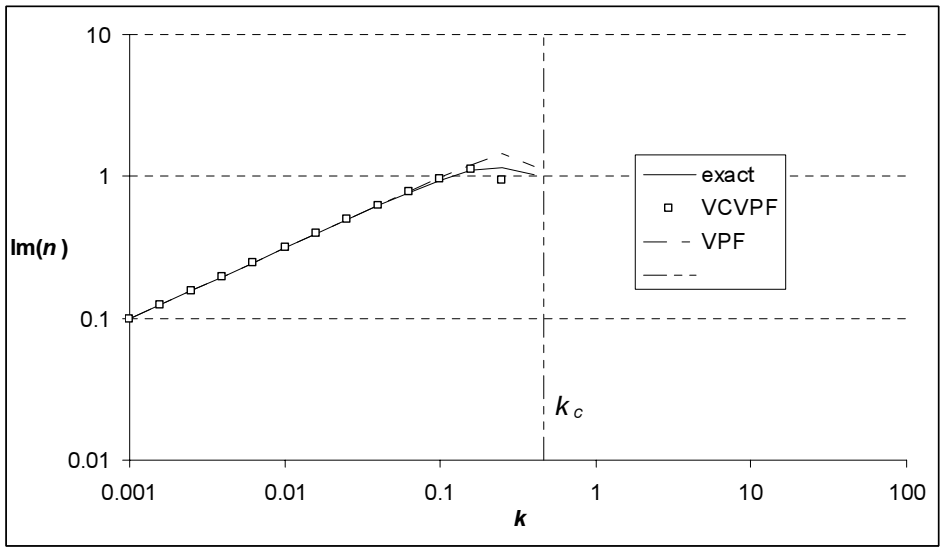

Figure 4. (c) Im(n), i.e. wave-velocity multiplied by k, vs. wave number k for ν =10 m^2/s. Im(n) is computed for the exact solution from (33), for VPF from (37) and for VCVPF from (42). When $k < k_c$, the three theories give almost the same wave-velocity. When $k > k_c$, all the three theories give zero imaginary part of n.

5. Comparison of the energy terms from the exact solution and from the potential part of the exact solution

The dissipation calculation by Lamb is based on the assumption that the kinetic energy, potential energy, and dissipation evaluated using the potential flow are reasonable approximations to the exact values. Such an assumption is also needed in the

VCVPF theory. We will compute the terms involved in the mechanical energy equation, changing rates of the kinetic energy and potential energy and the dissipation, in Lamb's exact solution and compare to the values evaluated using only the potential part of the exact solution.

The velocities in Lamb's exact solution are

$$u = (\mathrm{i}kA\mathrm{e}^{ky} - mC\mathrm{e}^{my})\mathrm{e}^{\mathrm{i}kx+nt} \quad , \quad \mathrm{v} = (Ak\mathrm{e}^{ky} + \mathrm{i}kC\mathrm{e}^{my})\mathrm{e}^{\mathrm{i}kx+nt} . \tag{47}$$

The changing rate of the kinetic energy in one wave period is

$$\overset{\circ}{\mathrm{K}} = \mathrm{dKEdt} = \frac{\mathrm{d}}{\mathrm{d}t}\int_V \rho|\mathbf{u}|^2/2\,\mathrm{d}V = \frac{\rho}{2}\frac{\mathrm{d}}{\mathrm{d}t}\int_{-\infty}^{0}\int_0^{\lambda}(u\overline{u}+\mathrm{v}\overline{\mathrm{v}})\,\mathrm{d}x\mathrm{d}y$$

$$= \frac{\rho}{2}(n+\overline{n})\lambda\mathrm{e}^{(n+\overline{n})t}\left[k|A|^2 - \frac{\mathrm{i}k\overline{m}A\overline{C}}{k+\overline{m}} + \frac{\mathrm{i}km\overline{A}C}{k+m} + \frac{|m|^2|C|^2}{m+\overline{m}} - \frac{\mathrm{i}k^2A\overline{C}}{k+\overline{m}} + \frac{\mathrm{i}k^2\overline{A}C}{k+m} + \frac{k^2|C|^2}{m+\overline{m}}\right], \tag{48}$$

where the overbar denotes conjugate variables. The elevation of the free surface η is obtained from the kinematic condition $\partial\eta/\partial t = \mathrm{v}$ at $\mathrm{y} \approx 0$ and it is

$$\eta = \frac{k}{n}(A + \mathrm{i}C)\mathrm{e}^{\mathrm{i}kx+nt} . \tag{49}$$

It follows that the changing rate of the potential energy in one wave period is

$$\overset{\circ}{\mathrm{P}} = \mathrm{dPEdt} = \frac{\mathrm{d}}{\mathrm{d}t}\int_0^{\lambda}\rho g\eta^2/2\,\mathrm{d}x = \frac{\rho g}{2}\frac{\mathrm{d}}{\mathrm{d}t}\int_0^{\lambda}\eta\overline{\eta}\,\mathrm{d}x$$

$$= \frac{\rho g}{2}(n+\overline{n})\lambda\mathrm{e}^{(n+\overline{n})t}\frac{k^2}{|n|^2}\left(|A|^2 - \mathrm{i}A\overline{C} + \mathrm{i}\overline{A}C + |C|^2\right). \tag{50}$$

Next we compute the dissipation

$$\int_V 2\mu\mathbf{D}:\mathbf{D}\,\mathrm{d}V = 2\mu\int_{-\infty}^{0}\int_0^{\lambda}\left(\mathrm{D}_{11}\overline{\mathrm{D}}_{11} + 2\mathrm{D}_{12}\overline{\mathrm{D}}_{12} + \mathrm{D}_{22}\overline{\mathrm{D}}_{22}\right)\mathrm{d}x\mathrm{d}y = 2\mu\lambda\mathrm{e}^{(n+\overline{n})t}\left[2k^3|A|^2 - \right.$$

$$\left.\frac{2\mathrm{i}k^3\overline{m}A\overline{C}}{k+\overline{m}} + \frac{2\mathrm{i}k^3m\overline{A}C}{k+m} + \frac{2k^2|m|^2|C|^2}{m+\overline{m}} - \frac{\mathrm{i}k^2\overline{m^2+k^2}A\overline{C}}{k+\overline{m}} + \frac{\mathrm{i}k^2(m^2+k^2)\overline{A}C}{k+m} + \frac{|m^2+k^2|^2|C|^2}{2(m+\overline{m})}\right]. \tag{51}$$

The constant C can be determined by the zero-shear-stress condition

$$\frac{C}{A} = \frac{2\mathrm{i}k^2}{m^2+k^2} . \tag{52}$$

Next we consider the changing rate of kinetic energy and potential energy and the dissipation evaluated using the potential part of the exact solution. This is done by putting $C = 0$ in (48), (50) and (51)

$$\overset{\circ}{\mathrm{K}} = \mathrm{dKEdt} = \frac{\rho}{2}(n+\overline{n})\lambda\mathrm{e}^{(n+\overline{n})t}k|A|^2 , \tag{53}$$

$$\overset{\circ}{\mathrm{P}} = \mathrm{dPEdt} = \frac{\rho g}{2}(n+\overline{n})\lambda\mathrm{e}^{(n+\overline{n})t}\frac{k^2}{|n|^2}|A|^2 , \tag{54}$$

$$\int_V 2\mu\mathbf{D}:\mathbf{D}\,\mathrm{d}V = 2\mu\lambda\mathrm{e}^{(n+\overline{n})t}2k^3|A|^2 . \tag{55}$$

We compute the expressions (48), (50) and (51), then compare them to (53), (54) and (55) in graphs. It should be noted that the values in the graphs are computed using the above expressions normalized by $\rho\lambda e^{(n+\bar{n})t}|A|^2$. $\overset{\circ}{\mathrm{K}}$ and $\overset{\circ}{\mathrm{P}}$ are negative and values plotted are their magnitudes. In figure 5, we plot $\overset{\circ}{\mathrm{K}}$ and $\overset{\circ}{\mathrm{P}}$ computed from (48), (50), (53) and (54), against the wave-number for glycerin and SO10000 oil; the dissipations computed using (51) and (55) are plotted in figure 6.

When k is small, the kinetic energy and potential energy are almost the same, which is a fact used by Lamb in his dissipation calculation. Figures 5 and 6 show that the potential part gives excellent approximations to dKEdt, dPEdt and dissipation computed from the exact solution. This is consistent with our observation that the dissipation method and VCVPF give good approximations to the exact solution when k is small.

When k is close to k_c, there are noticeable discrepancies between the results from the potential part and the exact solution. We observe in figures 1-4 that the agreement between the exact solution and VCVPF is poor near k_c.

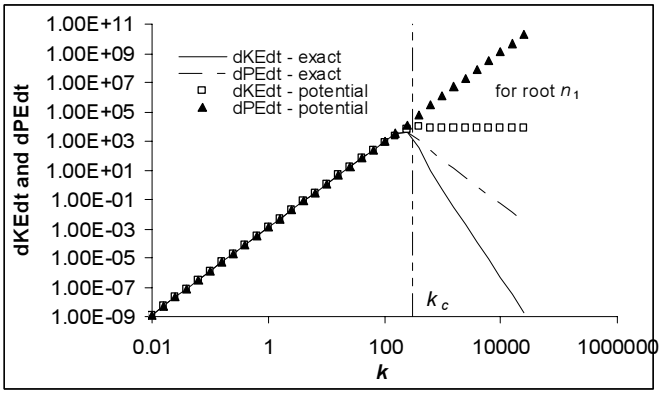

(a) Glycerin

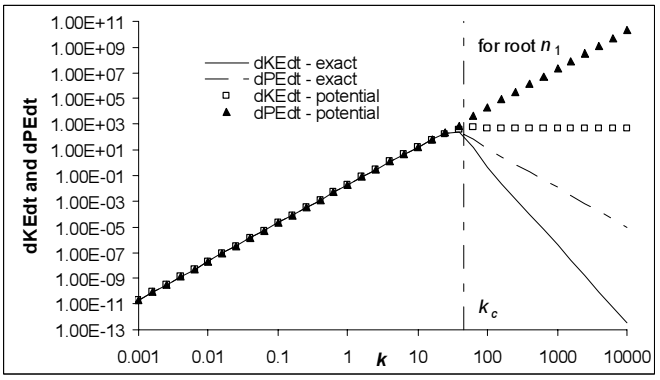

(b) SO10000 oil

Figure 5. $\overset{\circ}{\mathrm{K}}$ and $\overset{\circ}{\mathrm{P}}$ vs. k for (a) glycerin, $\nu = 6.21\times10^{-4}$ m^2/s (b) SO10000 oil, $\nu = 1.03\times10^{-2}$ m^2/s. The expressions for $\overset{\circ}{\mathrm{K}}$ and $\overset{\circ}{\mathrm{P}}$ are given by (48) and (50) for Lamb's exact solution, and are given by (53) and (54) for the potential part of the exact solution. The values in the graphs are computed using the above expressions normalized by $\rho\lambda e^{(n+\bar{n})t}|A|^2$. $\overset{\circ}{\mathrm{K}}$ and $\overset{\circ}{\mathrm{P}}$ are negative; the plotted values are their magnitudes. When $k < k_c$, the potential part gives excellent approximation to the exact solution; when $k > k_c$, the values of $\overset{\circ}{\mathrm{K}}$ and $\overset{\circ}{\mathrm{P}}$ associated with the root n_1 are plotted and the results from the potential

part do not agree with those from the exact solution.

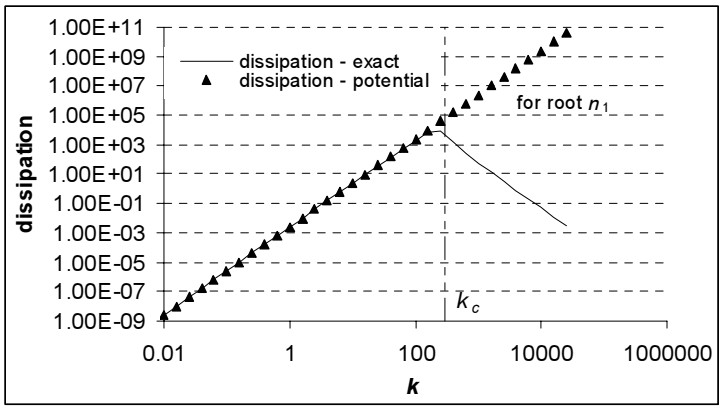

(a) Glycerin

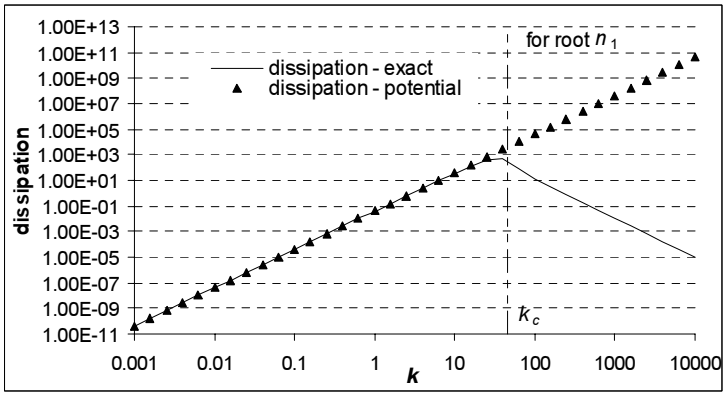

(b) SO10000 oil

Figure 6. The dissipation given by (51) for the exact solution and by (55) for the potential part of the solution as a function of the wave-number k for (a) glycerin, $\nu = 6.21\times10^{-4}$ m^2/s (b) SO10000 oil, $\nu = 1.03\times10^{-2}$ m^2/s. The values in the graphs are computed using the above expressions normalized by $\rho\lambda e^{(n+\bar{n})t}|A|^2$. When $k < k_c$, the potential part gives excellent approximation to the exact solution. When $k > k_c$, the agreement associated with the root n_1 is poor.

When k is larger than k_c, the energy and dissipation have two values corresponding to the two real roots for n. Since the smaller decay rate n_1 is more important, only the values of $\overset{\circ}{\mathrm{K}}$ and $\overset{\circ}{\mathrm{P}}$ and the dissipation associated with n_1 are plotted. The exact solution shows that $\overset{\circ}{\mathrm{K}}$ and $\overset{\circ}{\mathrm{P}}$ are different; but both of them decrease towards zero as k increases. The dissipation from the exact solution also approaches zero as k increases. These results are expected because the flow at the limit of large k represents "a slow creeping of the fluid towards a state of equilibrium with a horizontal surface" (Lamb 1932). The values of $\overset{\circ}{\mathrm{K}}$ and $\overset{\circ}{\mathrm{P}}$ for the root n_1 computed from the potential part of Lamb's exact solution do not agree with values computed from his complete solution in which the vortical part is included. This result may explain why the decay rate from VCPVF, which is based on the mechanical energy equation, does not agree well with the exact solution when k is large. However, this result does not mean that the vorticity is important. Lamb pointed out $m \approx k$ when k is large, which is confirmed in our calculation (see figure 7). Therefore the vorticity induced by the ψ part of the exact solution is

$$\nabla^2\psi = (m^2 - k^2)Ce^{my+ikx+nt} \approx 0\,. \tag{56}$$

This indicates that the ψ part is actually nearly irrotational when k is large. The result that the wave is nearly irrotational for large k was also pointed out by Tait (1890). Consequently, the decay rate from $-g/(2\nu k)$ VPF is in good agreement with the exact solution and no pressure correction is needed.

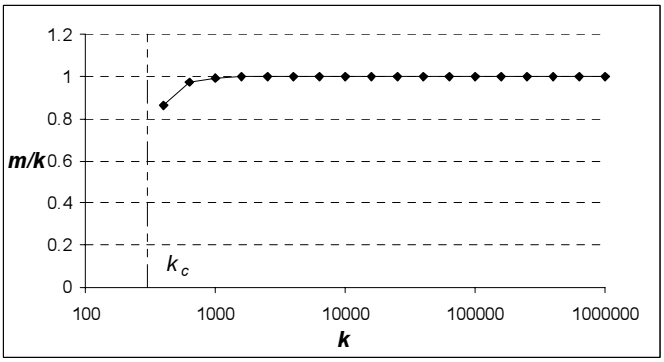

(a) Glycerin

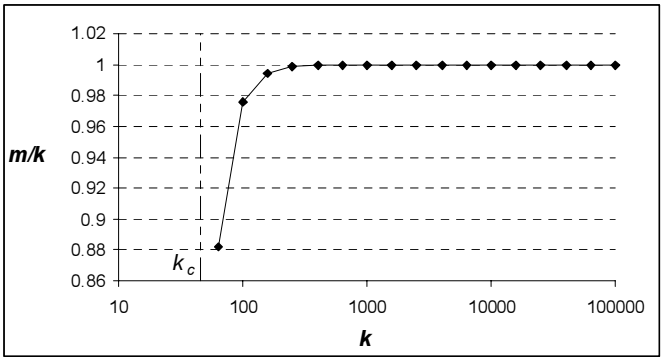

(b) SO10000 oil

Figure 7. The ratio m/k for $k > k_c$ for (a) glycerin, $\nu = 6.21\times10^{-4}$ m^2/s (b) SO10000 oil, $\nu = 1.03\times10^{-2}$ m^2/s. Only the value of m associated with the root n_1 is plotted. The plot shows that $m \approx k$ when k is large, indicating that the flow is nearly irrotational at large values of k.

5. Conclusion

- The problem of decay of free gravity waves due to viscosity was analyzed using two different theories of viscous potential flow, VPF and VCVPF.
- The contribution of the viscous part of the normal stress at the gas liquid surface is computed on the potential flow in VPF; otherwise the theory is the same as the irrotational theory of flow of an inviscid fluid.
- VCVPF is the same as VPF except for an additional viscous contribution to the pressure selected so as to remove the power of the uncompensated irrotational shear traction from the power of the traction terms arising in an energy analysis of the irrotational flow.
- The pressure correction leads to a hierarchy of potential flows in powers of viscosity. These higher order contributions vanish more rapidly than the principal

correction which is proportional to μ. The higher order corrections do not have a boundary layer structure and may not have a physical significance.

- The irrotational theory is in splendid agreement with Lamb's exact solution for all wave numbers k except for those in a small interval around k_c where progressive waves change to monotonic decay. VCVPF agree with Lamb's solution when $k < k_c$ (progressive waves) and VPF agrees with Lamb's exact solution when $k > k_c$ (monotonic decay).
- The cutoff wave number $k_c = (g/\nu^2)^{1/3}$ decreases as the viscosity increases. In practice waves associated with different wave numbers may exist simultaneously. For very viscous fluids, k_c is small and the majority of the wave numbers are above k_c, therefore the motion of monotonic decay dominates; for less viscous fluids, the motion of progressive waves may dominate.
- There is a boundary layer of vorticity associated with the back and forth motion of the progressive waves. The confined vorticity layer has almost no effect on the solution except for k near k_c.
- There is no explicit pressure correction in the exact solution. The pressure correction in VCVPF is given by terms involving the potential part of Lamb's solution (different than VCVPF), the surface elevation in Lamb's solution (different than VCVPF) and the vortical part associated with the stream function in Lamb's solution. The vortical part is not dominant and the pressure correction is not primarily associated with a boundary layer [see (31) and Table 1].
- The analysis of capillary instability of liquid in gas (Wang, Joseph and Funada 2005) is very much like the analysis of the decay of free gravity waves. The purely potential flow analysis is in splendid agreement with Tomotika's (1935) exact solution which has no explicit dependence on viscous pressure. In the case of capillary instability, the best result is based on VCVPF because the short waves which give rise to a sluggish decay in Lamb's problem are stabilized by surface tension.

Reference

Bassett, A. B. *A treatise on Hydrodynamics* (Deighton, Bell and Co., London, 1888; reprinted by Dover, New York, 1961), Vol. 2, p. 310.

Joseph, D. D. and Wang, J. 2004 The dissipation approximation and viscous potential flow. *J. Fluid Mech.* **505**, 365 - 377.

Kang, I.S. and Leal, L.G. 1988 The drag coefficient for a spherical bubble in a uniform streaming flow. *Phys. Fluids* **31**, 233 – 237.

Moore, D.W. 1963 The boundary layer on a spherical gas bubble. *J. Fluid Mech*. **16**, 161 –176.

Lamb, H. 1932 *Hydrodynamics*, 6th edn. Cambridge University Press (Reprinted by Dover 1945).

Prosperetti, A. 1976 Viscous effects on small-amplitude surface waves. *Phys. Fluids* **19**, 195–203.

Tait, 1890 Note on Ripples in a Viscous Liquid, Proc. R. S. Edin. xvii. 110 [*Scientific Papers*, Cambridge, 1898 – 1900, ii. 313]

Tomotika, S. 1935 On the instability of a cylindrical thread of a viscous liquid surrounded by another viscous fluid. *Proc. Roy. Soc. London* **A 150**, 322–337.

Wang, J., Joseph, D.D. and Funada T. 2004 Pressure corrections for potential flow analysis of capillary instability of viscous fluids. *J. Fluid Mech*. **522**, 383–394.